Nucleation of He bubbles in amorphous FeBSi alloy irradiated with He ions

AUTHOR(S):

Xu, Q.; Sato, K.; Yoshiie, T.

CITATION:

Xu, Q. ...[et al]. Nucleation of He bubbles in amorphous FeBSi alloy irradiated with He ions. Philosophical Magazine Letters 2012, 92(10): 527-533

ISSUE DATE:

2012-05

URL:

http://hdl.handle.net/2433/175274

Nucleation of He bubbles in amorphous FeBSi alloy irradiated with He ions

Q. Xu, K. Sato and T. Yoshiie

Research Reactor Institute, Kyoto University, Osaka 590-0494, Japan

Abstract

It is interesting to investigate the formation of He bubbles in amorphous alloys because point defects do not exist in amorphous materials. In the present study, the microstructural evolution of amorphous $Fe_{79}B_{16}Si_5$ alloy, either irradiated with 5 keV He^+ ions or implanted with 150 eV He^+ ions without causing displacement damage, and then annealed at a high temperature, was investigated using transmission electron microscopy (TEM). Vacancy-type defects were formed in the amorphous alloy after irradiation with 5 keV He^+ ions, and He bubbles formed during annealing the irradiated samples at high temperature. On the other hand, for samples implanted with 150 eV He^+ ions, although He atoms are also trapped in the free volume, no He bubbles were observed during annealing the samples even up to 873 K. In conclusion, the formation of He bubbles is related to the formation and migration of vacancy-type defects even in amorphous alloys.

1. Introduction

Atoms can be displaced by particles with high energy, such as neutrons, ions and electrons, in not only crystalline but also amorphous materials. A crystalline phase can be transformed into an amorphous phase under irradiation [1], especially in intermetallic compounds, as a consequence of irradiation damage [2-7]. On the contrary, irradiation with high-energy particles can induce nanocrystallization of an amorphous phase in metallic glasses, owing to irradiation-induced increases in the short-range order and in the atomic diffusivity [8-12]. Point defects are formed when atoms are displaced in crystalline materials. The aggregation of defects by diffusion of point defects induces microstructural evolution, which affects physical and mechanical properties of materials. Although point defects do not exist in amorphous material, damage is produced during irradiation with high-energy particles

With advances in nuclear power technology - fusion reactor technology in particular - interest in the behavior of He in solids has increased. He is generated in materials by the nuclear reaction of (n, α), which increases with increasing neutron energy. In addition, He is also introduced directly into plasma-facing materials (PFMs) by the He plasma in fusion reactors. He, which has a strong interaction with vacancies [13, 14], forms a high density of bubbles. In a fusion reactor, He and He bubbles lead to surface damage such as erosion, sputtering, and blistering of the plasma-facing materials. The impurity induced by erosion of PFMs is a key factor in the radioactive power loss of the plasma. Therefore, it is important to find materials with low He retention and/or better resistance to He bubble formation.

The crystal structure is one factor influencing the retention of He in solids, and amorphous metals have quite different atomic configurations from crystalline metals. It has

been reported that vacancy-type defects and He bubbles are formed in amorphous FeBSi and Fe-Ni-Mo-B alloy, respectively, during He irradiation [15-19]. He bubbles are formed by migrations of vacancies and He in crystalline metals and alloys. It is expected that vacancy-type defects and He are also mobile even in amorphous alloys; however, the formation process of He bubbles is not clear. In the present study, the formation process of He bubbles in amorphous alloys was investigated.

2. Experimental procedure

The amorphous alloy $Fe_{79}B_{16}Si_5$ (Metglas 2605S-3) was obtained in the form of sheets 25 μm thick, which was prepared by contact with a simple copper roller in an atmosphere of argon. The crystallization temperature (T_C) of the as-quenched $Fe_{79}B_{16}Si_5$ alloy was ~ 788 K. Crystalline FeBSi alloy specimens were prepared in a vacuum furnace by rapidly heating amorphous ribbons to 923 K for 0.5 h. The amorphous and crystalline samples were irradiated with 5 keV He^+ ions using an Omegatron gun, in which mono-energetic He^+ ions were collimated and mass-analyzed, at a flux of 5.0×10^{17} He^+/m^2 s. The irradiation dose was 1.0×10^{20} He^+/m^2. The displacement damage region was 50 nm from the incident surface, and the peak of displacement damage was 15 nm according to the calculations using the TRIM code [20], where the threshold displacement energy in FeBSi amorphous alloy was assumed to be 40 eV. The displacement damage and He concentration in the peak region were 1 dpa (displacements per atom) and 0.04, respectively. In addition, He implantation with a low energy (150 eV), without causing displacement damage, was carried out on amorphous alloy. The results of He thermal desorption from amorphous and crystalline FeBSi irradiated and implanted with 5 keV and 150 eV He^+ ions, respectively, show that He peaks appear in the samples [21]. After irradiation, isochronal annealing and

isothermal annealing experiments were carried out, and the microstructures of the amorphous and crystalline FeBSi samples were investigated using transmission electron microscopy (TEM).

3. Results

Figures 1 and 2 show the microstructural evolution in unirradiated and 5 keV He^+-irradiated amorphous $Fe_{79}B_{16}Si_5$ alloy during isochronal annealing from 300 to 773 K. Electron selected-area diffraction (SAD) patterns are also shown in the figures. Isochronal annealing experiments on the irradiated sample were carried out for 10 min in 50 K increments from room temperature using the heating stage of the TEM. The SAD patterns, consisting of halo rings, are characteristic of amorphous materials. In both cases, the microstructures and SAD patterns do not change until the temperature was increased to 623 K, i.e. no nanocrystalline particles were observed and the SAD patterns confirmed the amorphous phase. After annealing at 673 K for 10 minutes however, embedded nanoparticles were observed in the amorphous alloy, via diffraction spots corresponding to crystalline phases together with halo rings corresponding to the amorphous phase. The experimental results indicate that nucleation of crystals in amorphous alloy $Fe_{79}B_{16}Si_5$ begins at 673 K. With increasing annealing temperature to 773 K, the number of diffraction spots and hence nanoparticles increase.

Figure 3 shows the microstructural evolution in the 5 keV He^+-irradiated amorphous alloy during annealing at 673 K. As shown in Figure 1, embedded nanoparticles are observed after annealing the sample at 673 K for 10 min. The number of nanoparticles does not change very much even after annealing at 673 K for 80 minutes. After annealing

at 673 K for 200 minutes, an uneven distribution of He bubbles with an average size of about 5 nm are observed.

Figure 4 shows the microstructural evolution in 5 keV He^+-irradiated crystalline FeBSi during annealing from 300 to 973 K, in increments of temperature from 300 K to 50 K, with heating times of 10 min. He bubbles are observed on grain boundaries only after annealing at 973 K for 10 minutes. A magnification of the microstructures is shown in figure 5. Most of the He bubbles are formed in areas where a grain boundary exists.

In order to investigate the formation of He bubbles in the amorphous alloy, a He implantation at 150 eV, which does not produce displacement damage, was carried. Figure 6 shows the microstructural evolution in the 150 eV He^+-irradiated amorphous alloy during annealing from 300 to 873 K. Compared with the unirradiated amorphous alloy as shown in figure 2, the temperature at which clearly visible embedded nanoparticles appear was not 673 K, but 723 K, and diffraction spots associated with nanoparticles were also observed by SAD. However, He bubbles were not observed even after annealing the sample to 873 K.

4. Discussion

The formation of He bubbles in metals and alloys is caused by the migration of vacancies and interstitial He atoms. Barnes et al investigated the formation of He bubbles for the first time [22]. They irradiated Cu by He ions with an energy of 38 MeV. No effects appeared immediately after irradiation, but, after heating to 1023 K, the sample showed bubbles in the He-rich zone. From this observation it was deduced that He alone is not able to form bubbles and that vacancies are required to provide the necessary space for expansion. Although point defects do not exist in amorphous materials, it is clear that vacancy-type defects can be formed by irradiation [21, 23]. It is considered that the

formation of He bubbles is caused by the migration of He atoms and vacancy-type defects in amorphous alloys.

The results as shown in figures 1 and 2 indicate that He irradiation cannot influence the structural relaxation and crystallization of an amorphous alloy. A conceivable reason is that the region of displacement damage occurred only near the surface in a narrow region. However, He bubbles were formed during annealing the He-irradiated amorphous samples as shown in figures 2 and 3. As previously mentioned, vacancy-type defects can be formed in amorphous alloys under He irradiation with 5 keV. It is clear that He bubbles were formed in the crystallized region of the sample as shown in figure 3, but they were not formed in the amorphous regions even though the samples were irradiated uniformly by the He^+ ions. Vacancy-type defects or vacancy-He-type clusters migrate during structural relaxation and form He bubbles. Compared with the sample irradiated with He at 5 keV, vacancy-type defects do not exist in the 150 eV He-implanted sample, although free volume exists in the amorphous alloy. In this case, He atoms are trapped in the free volume, but He bubbles do not form even after the structural relaxation has occurred. Comparing the SAD patterns for the annealed unirradiated sample and the annealed sample implanted by He ions with 150 eV, it is seen that in the latter case diffraction spots are observed clearly at 723 K, 50 K higher than the former case. The present results indicate that the crystallization temperature of amorphous alloys might increase by the trapping of He atoms in the free volume.

5. Conclusions

Nucleation of He bubbles in amorphous FeBSi alloy irradiated with He ions has been investigated. It is clear that the formation of vacancy-type defects and their migration are

key factors in the formation of He bubbles in this He-irradiated sample. In addition, He bubbles are formed after structural relaxation of the amorphous alloy.

References

[1] M.L. Swanson, J.R. Parsons and C.W. Hoelke, Rad. Eff. 9 (1971) p.249..

[2] N.Q. Lam and P.R. Okamoto, Mater. Res. Soc. Bull. May (1994) p.703.

[3] W.L. Johnson, Prog. Mater. Sci. 30 (1986) p.81.

[4] A.D. Kororaev and A.N. Tyumentsev. Russ. Phys. J. 37 (8) (1994) p.783.

[5] D.E. Luzzi and M. Meshii, Res. Mech. 21 (1987) p.207.

[6] C. Jaouen, Solid State Phen. 23-24 (1992) p.123.

[7] D.F. Pedraza, Metall. Trans. 21A (1990) p.1809.

[8] T. Nagase, Y. Umakoshi and N. Sumida, Mater. Sci. Eng. A 323 (2002) p.218.

[9] T. Nagase and Y. Umakoshi, Mater. Sci. Eng. A 343 (2003) p.13.

[10] R. Tarumi, K. Takashima and Y. Higo, Appl. Phys. Lett. 81 (2002) p.4610.

[11] T. Nagase and Y. Umakoshi, Mater. Trans. JIM 45 (2004) p.13.

[12] W. Qin, T. Nagase and Y. Umakoshi, Acta Mater. 57 (2009) p.1300.

[13] P. Klaver, E. Haddeman and B. Thijsse, Nucl. Instrum. and Meth. B 153 (1999) p.228.

[14] W.D. Wilson and R.A. Johnson, in: P.C. Gehlen, J.R. Beeler, R.I. Jaffee (Eds.), Interatomic Potentials and Simulation of Lattice Defects, Plenum, New York, 1972, p.375.

[15] H. Van Swygenhoven, J. Vanoppen and L.M. Stals, Phys. Stat. Sol. (a) 67 (1981) K5.

[16] H. Van Swygenhoven, J. Moens, J. Vanoppen and L.M. Stals, Scripta Met. 15 (1981) p.629.

[17] H. Van Swygenhoven, J. Vanoppen, G. Knuyt and L.M. Stals, Rad. Effects 67 (1982) p.11.

[18] H. Van Swygenhoven, L.M. Stals and G. Knuyt, J. Nucl. Mater. 118 (1983) p.125.

[19] Y.X. Wang, Q. Xu, T. Yoshiie and Z.Y. Pan, J. Nucl. Mater. 376 (2008) p.133.

[20] J.P. Biersack, L.G. Haggmark, Nucl. Instrum. And Meth. 174 (1980) p.257.

[21] Q. Xu, X.Z. Cao, K. Sato, K. Mori and T. Yoshiie, Phil. Mag. Lett. 90 (2010) p.131.

[22] R.S. Barnes, G.B. Redding and A.H. Cottrell, Phil. Mag. 3 (1958) p.97.

[23] Q. Xu, X.Z. Cao, K. Sato, T. Iwai and T. Yoshiie, J. Phys.: Conf. Ser. 225 (2010) p.012059.

Figure Captions

Fig. 1 Microstructural evolution in unirradiated amorphous alloy $Fe_{79}B_{16}Si_5$ during isochronal annealing from 300 to 773 K. Diffraction spots, corresponding to crystalline phases, are observed after annealing at 673 K.

Fig. 2 Microstructural evolution in He-irradiated amorphous alloy $Fe_{79}B_{16}Si_5$ during isochronal annealing from 300 to 773 K. Diffraction spots, corresponding to crystalline phases, are observed after annealing at 673 K.

Fig. 3 Microstructural evolution in 5 keV He^+-irradiated amorphous alloy $Fe_{79}B_{16}Si_5$ during annealing at 673 K.

Fig. 4 Microstructural evolution in 5 keV He^+-irradiated crystalline alloy FeBSi during annealing from 300 to 973 K.

Fig. 5 Microstructural evolution in 5 keV He^+-irradiated crystalline alloy FeBSi during annealing at 973 K.

Fig. 6 Microstructural evolution in amorphous alloy $Fe_{79}B_{16}Si_5$ implanted He ions with 150 eV during isochronal annealing from 300 to 873 K. Diffraction spots, corresponding to crystalline phases, are observed after annealing at 723 K.

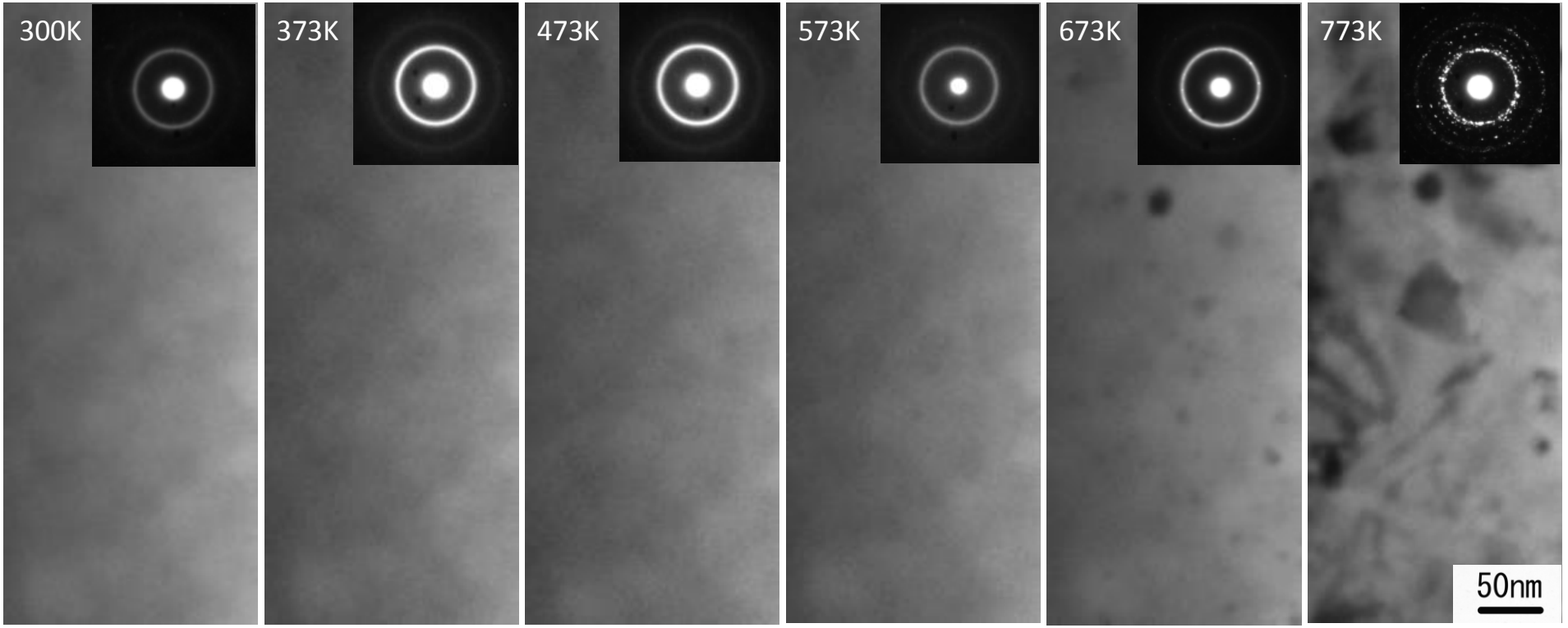

Fig. 1 Microstructural evolution in unirradiated amorphous alloy $Fe_{79}B_{16}Si_5$ during isochronal annealing from 300 to 773 K. Diffraction spots, corresponding to crystalline phases, are observed after annealing at 673 K.

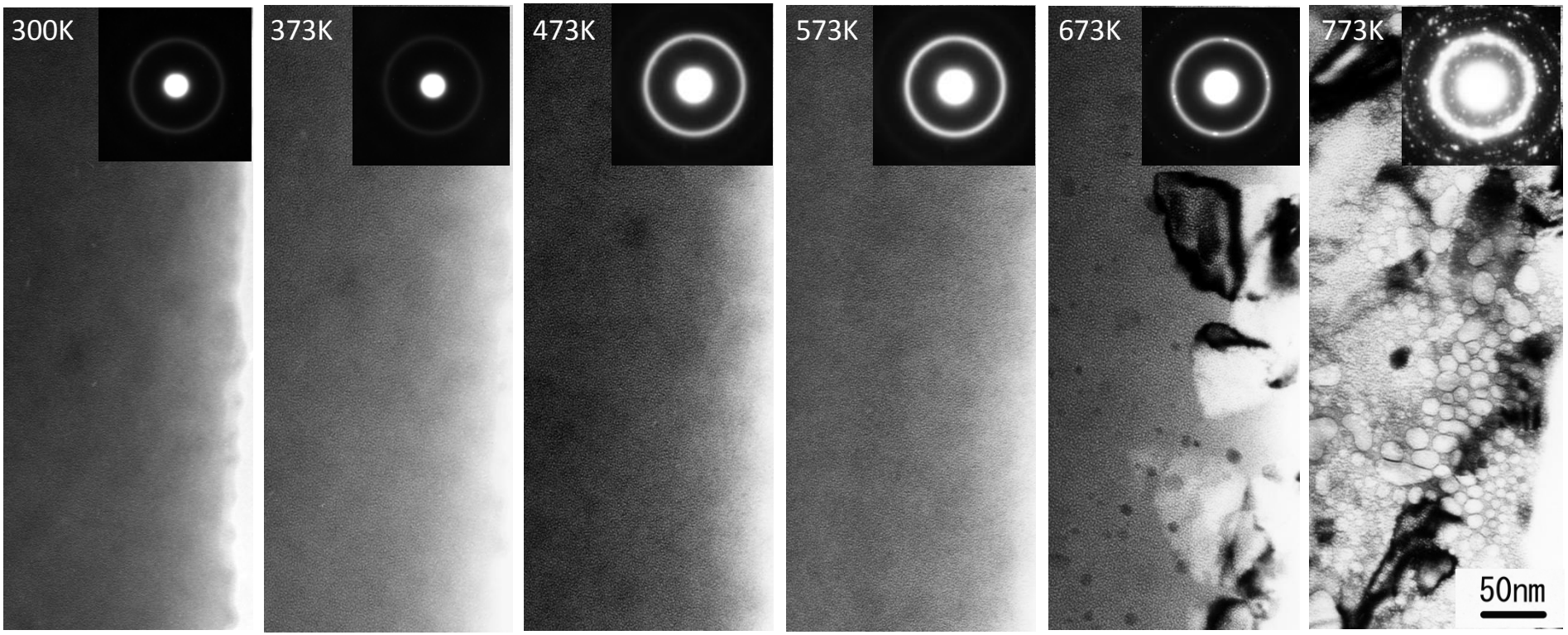

Fig. 2 Microstructural evolution in He-irradiated amorphous alloy $Fe_{79}B_{16}Si_5$ during isochronal annealing from 300 to 773 K. Diffraction spots, corresponding to crystalline phases, are observed after annealing at 673 K.

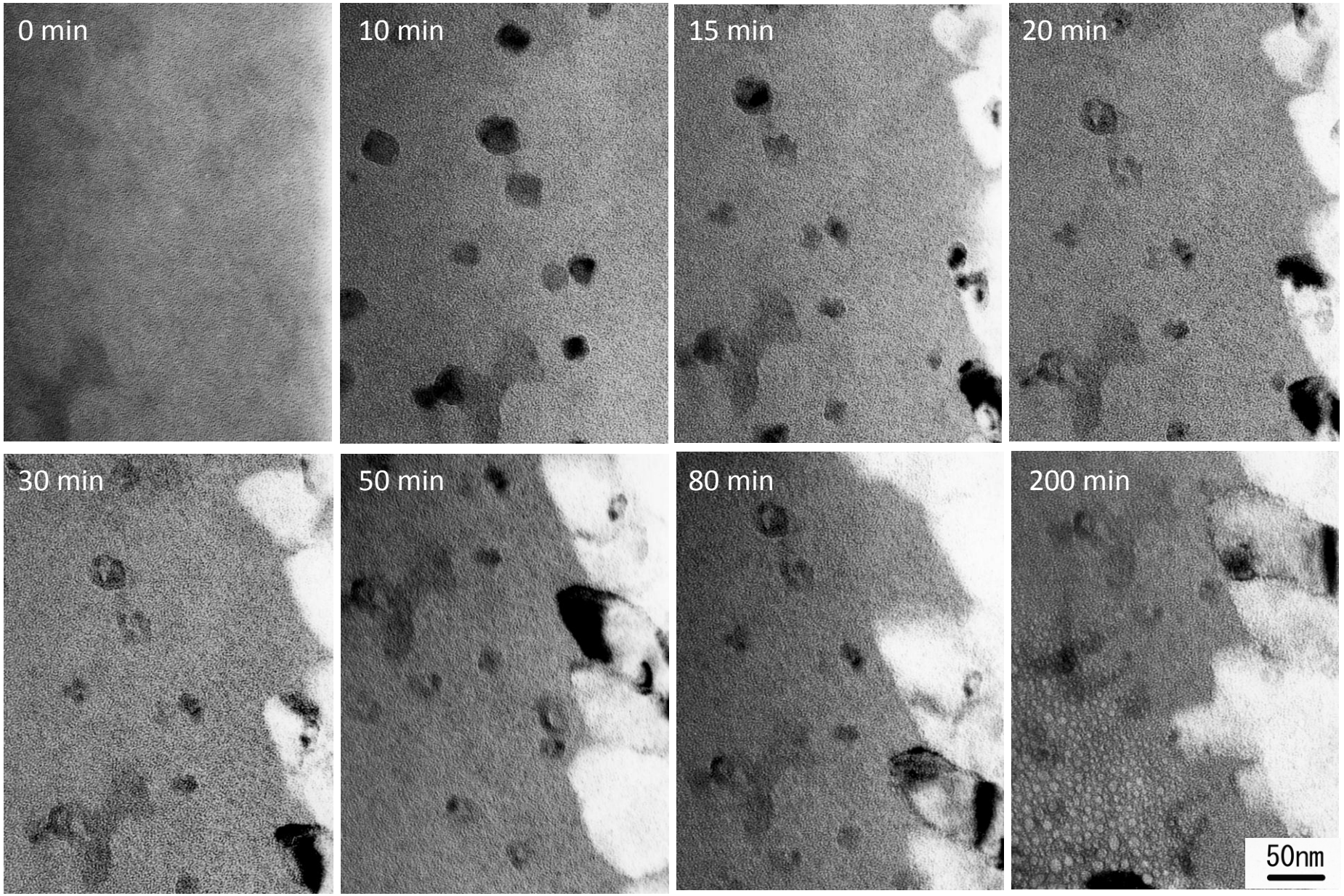

Fig.3 Microstructural evolution in 5 keV He^{+}-irradiated amorphous alloy $Fe_{79}B_{16}Si_5$ during annealing at 673 K.

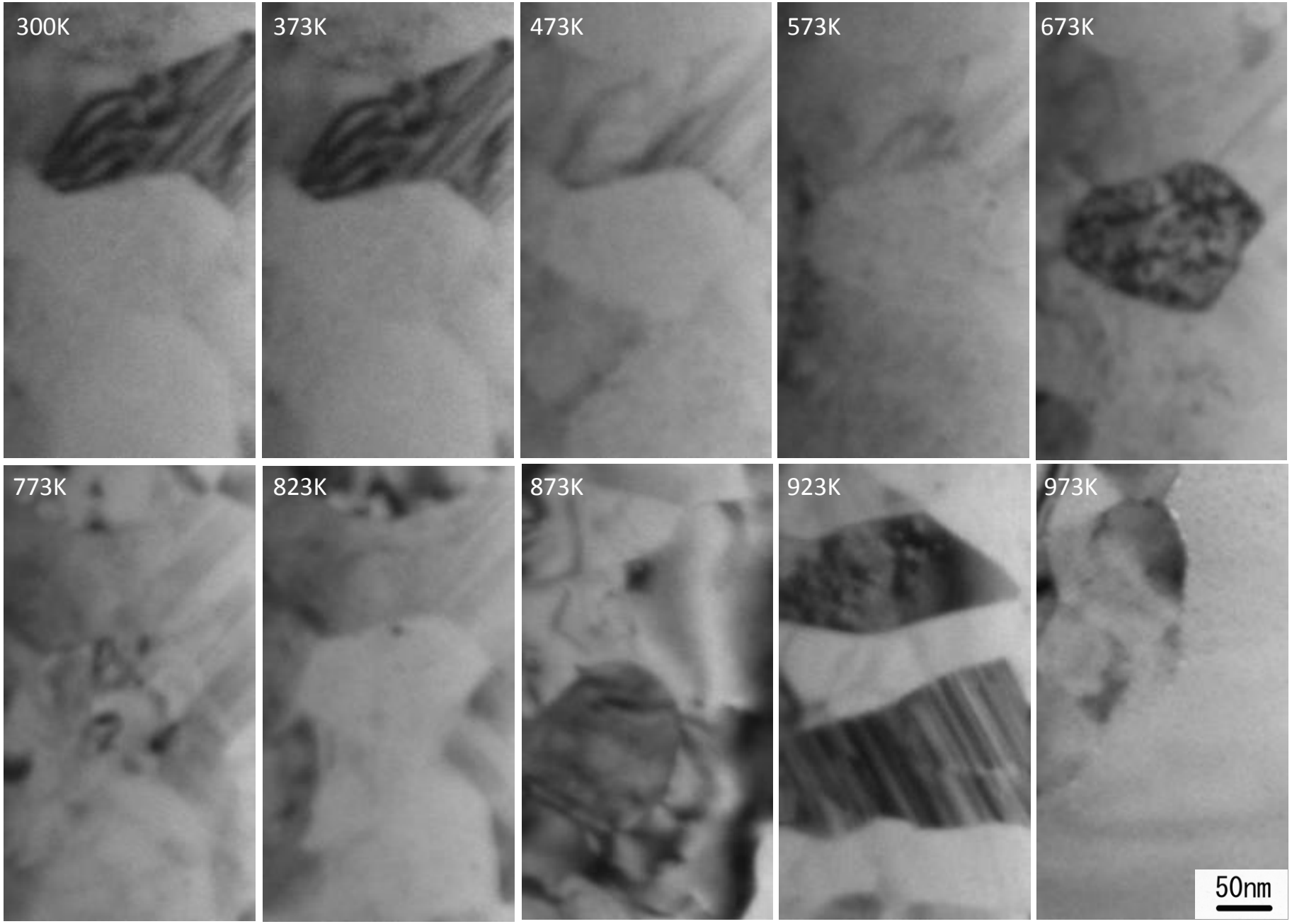

Fig.4 Microstructural evolution in 5 keV He^{+}-irradiated crystalline alloy FeBSi during annealing from 300 to 973 K.

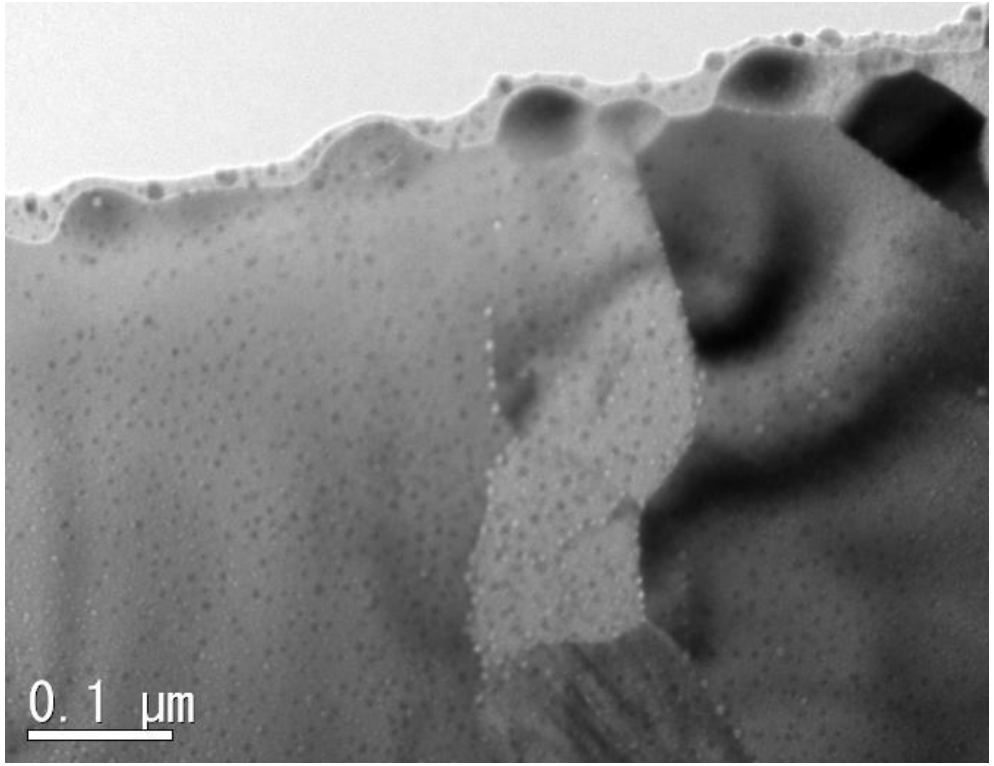

Fig.5 Microstructural evolution in 5 keV He^{+}-irradiated crystalline alloy FeBSi during annealing at 973 K.

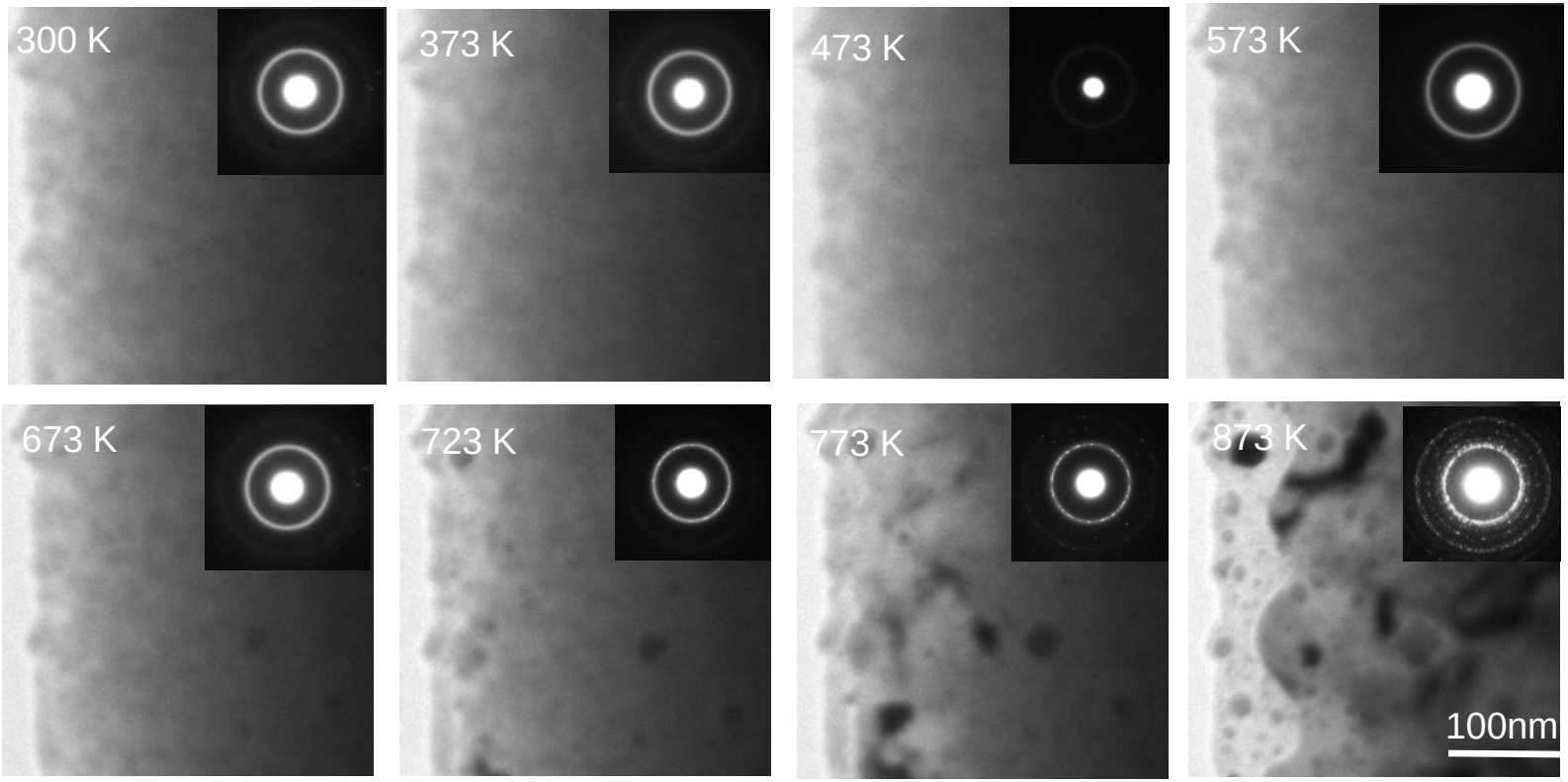

Fig. 6 Microstructural evolution in amorphous alloy $Fe_{79}B_{16}Si_5$ implanted He ions with 150 eV during isochronal annealing from 300 to 873 K. Diffraction spots, corresponding to crystalline phases, are observed after annealing at 723 K.